Anal. Bioanal. Electrochem., Vol. 16, No. 3, 2024, 258-268
https://www.doi.org/10.22034/abec.2024.712241

Analytical & Bioanalytical Electrochemistry

Full Paper

Single-Layered Zn-Fe Alloy Electrodeposition for The Protection of Mild Steel Structures

Ramesh S. Bhat,[1,*] and A. Chitharanjan Hegde[2]

[1]*Department of Chemistry, NMAM Institute of Technology, Nitte (Deemed to be University), Nitte-574110, Karnataka, India*
[2]*Electrochemistry Laboratory, Department of Chemistry, National Institute of Technology Karnataka, Srinivasnagar, 575025 India*

*Corresponding Author, Tel.: +91-8861037310
E-Mail: rameshbhat@nitte.edu.in

Received: 14 July 2023 / Received in revised form: 23 February 2024 / Accepted: 27 February 2024 / Published online: 31 March 2024

Abstract- Electrodeposition of Zinc-Iron alloy has been used to improve the corrosion resistance of mild steel. This alloy plating was successfully coated on mild steel using the electrodeposition technique. Under varied deposition conditions, the zinc-iron alloy films onto the steel plate were examined. The purpose of this study is to describe the corrosion characteristics of the coated sample in 3.5% NaCl for the application of novel, sacrificial coatings for the defence of steel structures. It has been thoroughly examined how plating variables including bath composition, pH, and current density affect the composition, morphology; and corrosion properties of the coatings were discussed. Scanning electron microscopy (SEM) and X-ray diffraction (XRD) are used to analyze the morphological characteristics and phase structure of the coatings. The surface roughness of the coating was measured by Atomic Force Microscopy (AFM). The Vickers indenter was employed to measure the microhardness of the coated sample. The corrosion resistance of Zn-Fe alloy coatings was assessed using electrochemical impedance spectroscopy (EIS) and polarization techniques at different current densities. The new low-cost Zn-Fe alloy coating was used for automobile applications.

Keywords- Corrosion; Electrodeposition; Microhardness; XRD; SEM; AFM

1. INTRODUCTION

Zinc and its alloys are widely used for electroplating steel sheets to provide corrosion resistance, mainly in the automobile industry. Under harsh climatic conditions, the corrosion resistance of pure zinc coating on steel is inadequate and unacceptable. For increased corrosion resistance and more cost-effective ways to protect steel sheets for longer periods under harsh atmospheric circumstances, a variety of techniques and materials, including various organic paints and zinc alloys, are being researched [1-3]. Numerous studies have been conducted on Zn alloy single-layer electroplated coatings, including Zn–Ni, Zn–Co, and Zn–Fe coatings [4–9]. Research has demonstrated that these coatings exhibit exceptional anti-corrosive qualities, including greater iron substrate protection from corrosion [9–14] and better tribological behaviour when compared to pure Zn electrodeposited coatings [15–17]. As a result, many industrial fields, including the automotive industry, have employed Zn alloy coatings. The coating should have consistent, smaller, and bright, grain size in order to achieve superior metallurgical characteristics. To obtain the bright deposit, some organic molecules are therefore necessary. Industrialists typically utilized a variety of organic substances to produce bright deposits in a single bath. Pollutant levels in the environment increase over time [18]. Electrodeposited Zn-Fe alloy containing 15-25% wt. Fe on steel can provide sacrificial protection to steel and serve as a viable substitute for zinc and cadmium coatings [19]. Zn-Fe alloys are deposited from acid sulphate, chloride, and sulphate-chloride baths [20]. Zinc–iron alloys exist in various phases, and their structure and morphology are also responsible for better corrosion resistance of a deposit [21].

In the present work, a wide current density range has been explored for the electrodeposition of Zn-Fe alloy coating from a sulphate solution. The deposit is produced through Hull cell studies with sulphamic acid present as a brightener. The concentration of the bath ingredient and the operation conditions are optimized. The effect of cathode current density on surface microstructure, CCE, chemical composition, corrosion resistance of the coating, thickness, phase structure, and hardness, were investigated, and results were discussed.

2. EXPERIMENTAL SECTION

2.1. Materials

Research-grade chemicals were purchased from Merck including zinc sulphate, ferrous sulphate, sodium chloride, citric acid, sodium acetate, and sulphamic acid.

2.2. Preparation of Solution:

Research-grade chemicals and distilled water were used to make the electroplating bath. Based on preliminary research, the pH of the electroplating solutions was set at 4, and as

needed, the pH was adjusted by adding diluted H_2SO_4 or KOH and measuring with a pH meter (HANNA-pH21). The electrolyte temperature was also kept constant at 30 °C.

2.3. Materials Preparation and Characterization

The mild steel sample (2.5 cm × 2.5 cm) was used as a cathode in this experiment. The cathode was cleaned with purified water, and trichloroethylene, then dried after finishing the surface with sandpaper with various grit sizes 200, 400, 600, 800, and 1200.

The bath component optimization was accomplished by using a conventional Hull cell. The polyvinyl chloride cell, which has a 100 mL capacity and anode and cathode distance of 4 cm, was used to develop the monolayer coating. A mild steel substrate served as the cathode and a pure Zn plate was used as an anode. All the depositions were accomplished galvanostatically by employing a DC power source to maintain a constant pH and temperature for ten minutes. The sulphamic acid was used as a brightener for the coatings. Citric acid was used as a buffer to keep the constant pH of the bath, and sodium acetate was added to make the conductivity of the bath. Table 1 shows the bath constituents for the coatings.

The electrochemical characteristics of the coatings were investigated using the potentiodynamic polarization (PP) method and electrochemical impedance spectroscopy (CH Instruments, Inc. Austin, USA). The three-electrode cell that makes up the potentiostat is utilized to conduct the electrochemical test. The working, counter, and reference electrodes were electroplated mild steel, platinum, and calomel, respectively. As a corrosive environment, a 3.5% sodium chloride solution was employed. The PP experiments were conducted at a scan rate of 0.01 mVs^{-1}, with the open circuit potential (OCP) ranging between ±0.200 mV. The potentiodynamic polarization approach was used to obtain the corrosion data [22]. Impedance was measured using sinewaves with a frequency range of 100 kHz to 10 MHz, a power of 10 mV, and an exposure time of 1 hour. After the corrosion test, the coating sample was examined using the scanning electron microscope (SEM, model -JEOL JSM-6380 LA, Japan) method. AFM, Nanosurf Flex AFM, Switzerland) was used to measure the surface roughness of the Zn-Fe alloy coatings. The hardness of coatings was measured using a Vickers microhardness tester (Clemex Tech USA Corp.). A colorimetric method was used to assess the compositions of the deposits. The percentage of cathode current efficiency (% CCE) of the plating can be calculated using the mass, and composition of the deposit [23].

3. RESULTS AND DISCUSSION

3.1. Optimization of Zn-Fe alloy bath

Zn-Fe alloy electrodepositions were formed using an acidic sulphate bath including $ZnSO_4$, $FeSO_4$, Citric acid, Sulphamic acid, and Ammonium chloride. Ammonium chloride was added to the bath to make it more conductive. A new Zn-Fe bath was optimized using the Hull cell

approach. All depositions were carried out by a direct current (DC) power supply. Each component is varied, and deposit patterns are scrutinized for their appearance. The bath composition and current density (CD) have been optimized based on the appearance of the coatings. The deposits were found in the range of 1.0-5.0 A/dm^2, varying from semi-bright to bright and finally flaky bright. Table 1 shows the optimized composition, bath parameters, and conditions of the plating.

Table 1. Bath constituents for the coatings

Bath composition	Amount (g/L)	pH - 4.0
$ZnSO_4$	30.0	Temperature- 30 °C
$FeSO_4$	15.0	Anode – Pure Zn
Citric acid	2.0	
$(NH_4)_2SO_4$	50.0	Cathode - Mild steel
Sulphamic acid	1.0	

3.2. Effect of current density (CD)

The CD has a significant impact on both the corrosion performance of the coating and the surface microstructure of the coatings. Table 2 shows how CD enhanced the weight percentage of Fe in the deposit. At low CD, the bath generated a blackish deposit; at high CD (5 A/dm^2), the bath produced a porous bright deposit. At ideal CD (3 A/dm^2), a sound deposit was found with 2.85% of Fe (Table 2). Therefore, in a wide range of C.D.s, the Zn-Fe alloy bath shows an abnormal co-deposition, and it was revealed that, at very low CD, the weight percentage of Fe in the deposit increased (Table 2). The rapid depletion of more readily depositable Zn^{2+} ions on the cathode surface led to the acceptance of the increase in weight percentage of Fe with CD [24,25]. Figure 1 shows the weight percentage of Fe in the deposit with CD.

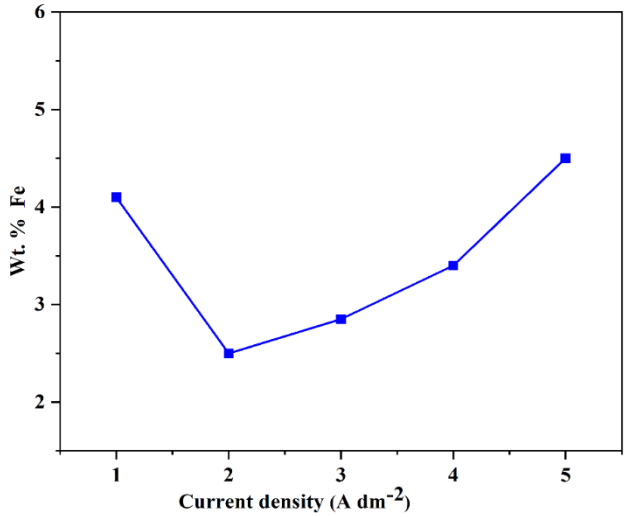

Figure 1. Weight % of Fe in Zn-Fe alloy film at various CDs

Table 2. Wt.% of Fe, CCE, hardness, thickness, and nature of deposit with current density

CD (A/dm^2)	*p*H	Wt.% Fe	CCE (%)	VH_{500}	Thickness (μm)	Nature of the deposit
1. 0	4.0	4.10	80.4	132	6.8	Blackish
2. 0		2.50	85.2	145	7.5	Semi bright
3. 0		2.85	89.1	159	10.3	Bright
4.0		3.40	93.0	167	11.9	Bright
5.0		4.50	92.6	162	13.0	Porous Bright

3.3. Hardness and Thickness and %CCE Analysis

It was found that the hardness of the coating film depends on the CD employed for deposition. Table 2 shows the microhardness of Zn-Fe coatings with CD. The hardness value increases with CD with a load of 500 g. It may be noted that at the low CD side, high iron content in the deposit, and the deposit showed less hardness. Where the diamond tip must have come into contact with the substrate during the measurement, it can be because of the thin coating. The hardness of the coating is found to increase with CD, and then decrease, as shown in Table 2. The decrease of hardness at very high CD may be due to the occlusion of metal hydroxide into the crystal lattice, caused by excessive liberation of hydrogen during plating [24]. The hardness of the Zn-Fe deposit increased with CD, as shown in Figure 2.

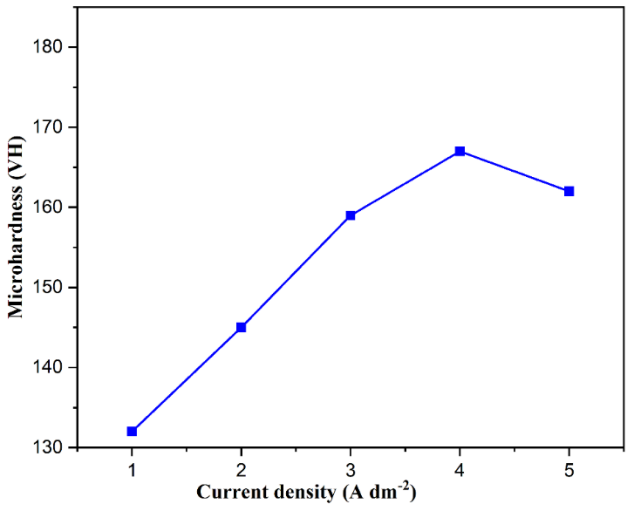

Figure 2. Vickers microhardness for the alloy coatings at different CDs

As observed in Table 2, the thickness of the deposit rises with CD. The observed linear dependence of thickness with CD may be due to the adsorbed metal hydroxide caused by the gradually rising pH because of the evolution of hydrogen gas. In all cases of deposition conditions, the CCE is high. i.e. > 80%. Generally, it was found that CCE decreased slightly as CD increased, which could result from excessive hydrogen evolution. Table 2 shows the impact of CD on the percentage of CCE. The higher porosity towards high CD could be the cause of it.

3.4. Polarization Analysis

Electroplated Zn-Fe alloy coatings developed at different CDs were subjected to corrosion study, and equivalent data are shown in Table 3. The polarization behaviors of the coatings are shown in Figure 3. The potentiometric polarization technique was carried out to determine the corrosion rate of the developed Zn-Fe coatings at CDs from 1 A/dm^2 to 5 A/dm^2. During the corrosion testing, the electrodes were immersed in the 3.5% NaCl solution as a corrosive medium and left at OCP for 10 minutes. Table 3 provides the corrosion data, including cathodic (βc), and anodic Tafel (βa), corrosion potential (E_{corr}), and corrosion current density (I_{corr}). The corrosion rate (CR) decreases with CD due to the change in phase structure brought on by the change in Fe concentration in the deposit. High Fe content is the cause of the high CR seen at very low current density. This could be a result of the tendency of the bath to go from abnormal to normal co-deposition. The coating developed at 3.0 A /dm^2 with 2.85 wt% Fe displayed the lowest corrosion rate, which was reported to be 0.110 mm/ year. Thus, it can be concluded that the addition of sulphamic acid at 3.0 A /dm^2 has decreased the availability of free Fe^{2+} ions in the solution by promoting correct complexation, coating homogeneity, and lowering the corrosion rate.

Table 3. Corrosion data for the alloy coatings at different CDs

CD (A/dm^2)	E_{corr} (V)	I_{corr} (μA/cm^2)	βc (1/V)	βa (1/V)	CR (mm/year)
1.0	-0.692	36.48	4.393	18.366	0.499
2.0	-0.679	15.34	6.264	11.264	0.218
3.0	-0.627	7.94	8.678	13.003	0.110
4.0	-0.662	22.48	6.971	9.408	0.335
5.0	-0.585	69.69	1.872	9.122	0.961

3.5. EIS Studies

Electrochemical impedance spectroscopy (EIS), a technique for studying corrosion resistance, is used to evaluate the characteristics and dynamics of the electrochemical process

occurring at the electrode/solution interface in corrosive solutions [26,27]. The EIS measurements are carried out for the films deposited from sulphate baths and to analyze the corrosion resistance behaviour of Zn-Fe coatings. The measured EIS data displayed as Nyquist are shown in Figure 4. The impedance module is noted to have a semicircle form. The capacitance of the oxide film is usually quite low, the impedance module of the MS-coated samples occurs in the high-frequency band, and their Nyquist plots show well-defended capacitive arcs. Thus, the low-frequency time constant should be connected to the activation process itself, whereas the high-frequency time constant might be linked to the generation of a porous oxide film.

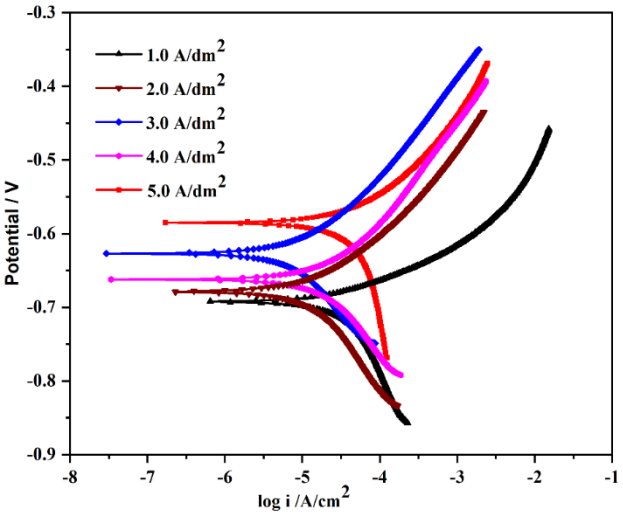

Figure 3. Polarization plot of Zn-Fe alloy coatings

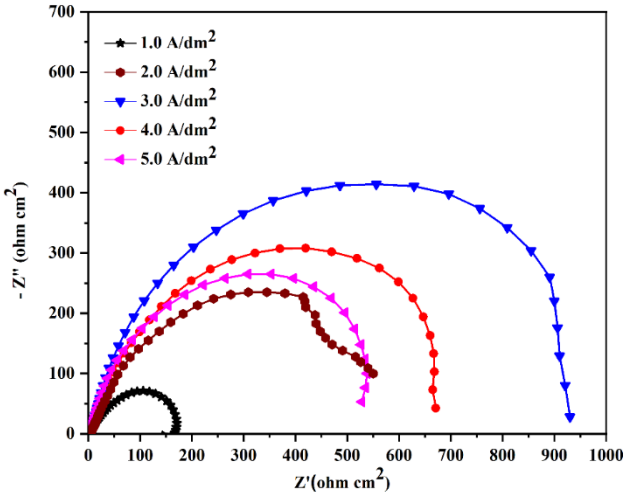

Figure 4. Nyquist plot for Zn-Fe alloy films

The improved corrosion resistance of the Zn–Fe alloy coating at an ideal current density of 3 A/dm^2 can be attributed to a larger coating capacitance, as seen by its noticeably larger impedance and larger diameter of the (in completed) semicircle. The dielectric constant and coating thickness have a direct relationship with the capacitive impedance at high frequencies. Because the Zn–Fe had a stronger corrosion resistance, this constant decreased. Low-level frequencies, on the other hand, are referred to as the electric double layer. The lower CD (1 A/dm^2) Zn-Fe coated sample shows a smaller impedance module may be due to a lower in the coating capacitance. But at higher CD (5 A/dm^2), the radius of the capacitive loop is decreased may be due to porous deposit.

3.6. Surface analysis

The surface topography (3D) of Zn–Fe alloy film has been examined by atomic force microscopy (AFM) technique. Figure 5 shows the AFM images of the Zn-Fe alloy film at the optimal CD (3 A /dm^2). The AFM image was used to determine the surface roughness of the film (Ra = 38.1 nm) and root-mean-square roughness (Zrms = 52.7 nm). As a result, it appears that the surface features of the alloy film are consistent, smooth textured, and have modest peaks that correspond to regular granule sizes. The alloy film thus showed a lower rate of corrosion at the optimal CD (3 A/dm^2) [28]. Using a scanning electron microscope, the surface morphology of the Zn-Fe alloy films was investigated (SEM). Figure 6, shows the SEM micrograph at 3 A/dm^2. It is noted that the deposit shows a smaller grain size, uniform, non-porous, and thin surface (Figure 6), and hence better corrosion resistance of the coatings [29].

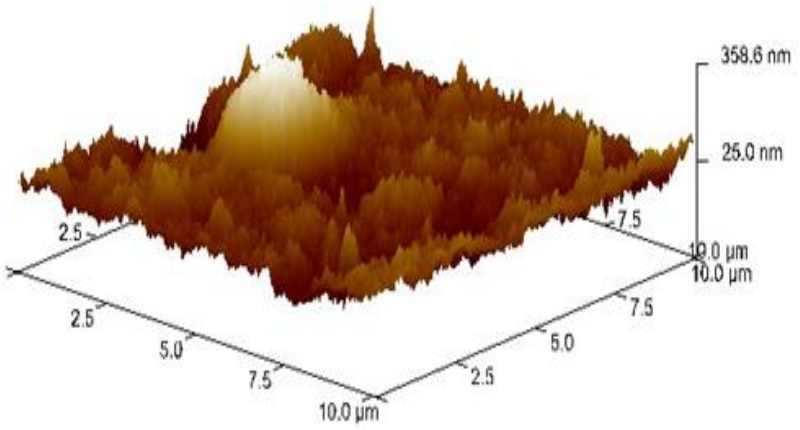

Figure 5. AFM image of Zn-Fe coating film

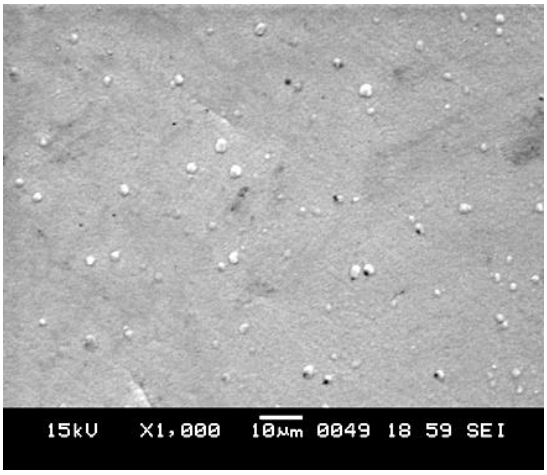

Figure 6. SEM image of Zn-Fe coating film (3 A/dm^2)

3.7. XRD Analysis

The X-ray Diffraction (XRD) patterns of the electrodeposited Zn-Fe alloys from the electrolytic bath are shown in Figure 2. As a result of their polycrystalline structure, the electrode-plated samples, and XRD measurements revealed that they each have a unique crystal orientation. The ideal orientation of XRD peaks is along the (100), (101), and (103) planes. The experimental parameters, such as pH, CD, and temperature, have an impact on the preferred crystal orientation of zinc electrodeposits. The Zn-Fe alloy coatings have the same structure as zinc [30] but a distinct crystallographic orientation because of the minor quantity of iron. Depending on the chemical compositions, the phases of the electrodeposited Zn-Fe alloy are quite complex [31].

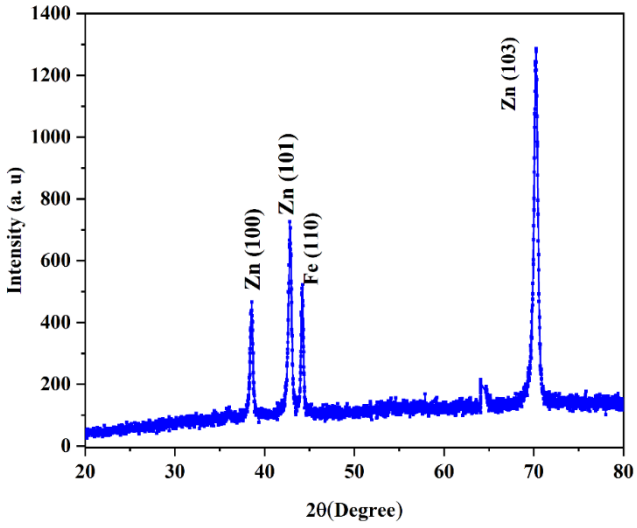

Figure 7. XRD plot of Zn-Fe coating at (3 A/dm^2)

All the examined deposits have reflections of the zinc-rich phase (JCP: 4-0831) [32]. The Zn-Fe alloys that are electrodeposited exhibit metastable structures and coexist in a variety of phases throughout a broad range of compositions. As the Zn content in the deposits increases, the signals belonging to the η phase become more intense.

4. CONCLUSION

The aim of the present investigation was to increase the corrosion resistance property of the coating by optimizing the parameters involved in the Zn-Fe alloy coating. Bright and homogeneous deposits are seen in the coating at optimal CD (3 A/dm^2). The optimal current density of 3.0 A/dm^2 was found to result in a CR of 0.110 mm/year. The AFM study indicates that the coating surface is homogeneous, less coarse, and dense and the predominance of small peaks with regular grain size helps to minimize the rate of corrosion. The Zn (101) and Zn (103) significant phases were shown to be responsible for the improved corrosion resistance of the coating, according to the XRD results. The topography and surface roughness of Zn-Fe alloy have been shown using AFM and SEM examination. There has been a discussion of the relationship between corrosion resistance and surface morphology. The results show that Zn–Fe alloy coatings with extremely low environmental corrosion rates have better corrosion-resistant properties. Thus, the alloy film under investigation can serve as a layer that prevents corrosion on a variety of industrial items (machinery tools, and equipment).

Declarations of interest

The authors declare no conflict of interest in this reported work.

REFERENCES

[1] N. Kanani, Electroplating: Basic Principles Processes and Practice, Elsevier Ltd, Berlin, (2006).
[2] R. Bhat, S. Bekal, and A.C. Hegde, Anal. Bioanal. Electrochem. 10 (2018) 1562.
[3] R. Bhat, K.U. Bhat, and A.C. Hegde, Prot. Met. Phys. Chem. Surf. 47 (2011) 645.
[4] S. Yogesha, and A.C. Hegde, J. Mater. Process. Technol. 211 (2011) 1409.
[5] V. Thangaraj, K. Ravishankar, and A.C. Hegde, Chin. J. Chem. 26 (2008) 1.
[6] K.K. Lee, I.H. Lee, C.R. Lee, and H.K. Ahn, Surf. Coat. Technol. 201 (2007) 6261.
[7] Z. N. Yang, Z. Zhang, and J.Q. Zhang, Surf. Coat. Technol. 200 (2006) 4810.
[8] N. Boshkov, K. Petrov, D. Kovacheva, S. Vitkova, and S. Nemska, Electochim. Acta 51 (2005) 77.
[9] R.S. Bhat, Fabrication of Multi-Layered Zn-Fe Alloy Coatings for Better Corrosion Performance. In Liquid Metals, Open Tech: Singapore (2021).
[10] J. Fei, and G.D. Wilcox, Surf. Coat. Technol. 200 (2005) 3533.

[11] R.S. Bhat, and A.C. Hegde, Trans. Inst. Met. Finish. 93 (2015) 157.
[12] R.S. Bhat, M.K. Balakrishna, P. Parthasarathy, and A.C. Hegde, Coatings 13 (2023) 772.
[13] R.S. Bhat, K. Venkatakrishna, J. Nayak, and A.C. Hegde, J. Mater. Eng. Perform. 29 (2021) 6363.
[14] R.S. Bhat, P. Nagaraj, and S. Priyadarshini, Surf. Eng. 37 (2021) 755.
[15] R.S. Bhat, R. Udupak, and A.C. Hegde, J. Metals, Materials and Minerals 20 (2017) 1.
[16] R.S. Bhat, and A.C. Hegde, Anal. Bioanal. Electrochem. 6 (2014) 606.
[17] R. S. Bhat, K. Venkatakrishna, and A.C. Hegde, Anal. Bioanal. Electrochem. 15 (2023) 90.
[18] R. Bhat, and A.C. Hegde, J. Electrochem. Sci. Eng. 9 (2019) 9.
[19] Y. Arthoba Naik, and T.V. Venkatesha, Bull. Mater. Sci. 28 (2005) 495.
[20] H. Nakano, S. Arakawa, S. Oue, and S. Kobayashi, Mat. Tran. 56 (2015) 1664.
[21] K.O. Nayana, T.V. Venkatesha, and K.G. Chandrappa, Sur. Coat. Tech. 235 (2013) 461.
[22] H. Park, and J.A. Szpunar, Corr. Sci. 40 (1998) 525.
[23] R. S. Bhat, K.B. Manjunatha, R. Prasanna Shankara, K. Venkatakrishna, and A.C. Hegde, Appl. Phys. A: Mater. Sci. Process. 126 (2020) 772.
[24] A. Brenner, Electrodeposition of Alloys: Principles and Practice; Academic Press: New York, NY, USA (1963) pp. 589.
[25] R.S. Bhat, K. Venkatakrishna, and A.C. Hegde, Anal. Bioanal. Electrochem. 15 (2023) 90.
[26] M.K. Punith Kumar, T.V. Venkatesha, M.K. Pavithra, and A.N. Shetty, Synth. React. Inorganic Met. Nano-Metal Chem. 42 (2012) 1426.
[27] S. Fashu, C.D. Gu, J.L. Zhang, M.L. Huang, X.L. Wang, and J.P. Tu, Nonferrous Met. Soc. China (English Ed.) 25 (2015) 2054.
[28] S. Anwar, F. Khan, and Y. Zhang, Saf. Environ. Prot. 141 (2020) 366.
[29] I.H. Karahan, Chin. J. Phys. 46 (2008) 105.
[30] R. Fratesi, G. Lunazzi, and G. Roventi, in: Organic and Inorganic Coatings for Corrosion Prevention, Vol. 20, Eds. L. Fedrizzi, and P.L. Bonora, the Institute of Materials, London (1997) pp. 130.
[31] V.B. Miskovic-Stankovic, J.B. Zotovic, Z. KacarevicPopovic, and M.D. Maksimovic, Electrochim. Acta 44 (1999) 4269.
[32] J.B. Bajat, Z. Kacarevic-Popovic, V.B. MiskovicStankovic, and M.D. Maksimovic, Prog. Org. Coat. 39 (2000) 127.